Some Statistics of Lagrangian and Eulerian Wind Fluctuations

STEVEN R. HANNA

Air Resources Atmospheric Turbulence and Diffusion Laboratory, NOAA, Oak Ridge, TN 37830

(Manuscript received 19 July 1978, in final form 11 December 1978)

ABSTRACT

The linear relationship $u'(t+\tau)=u'(t)R(\tau)+u''(t)$ is shown to be approximately valid for Lagrangian and Eulerian wind speed observations in the planetary boundary layer, where t represents any time and $t+\tau$ is some later time, u' is the turbulent wind speed fluctuation, $R(\tau)$ the autocorrelation coefficient, and u'' a random wind speed component assumed to be independent of u'. Eulerian wind data from the Minnesota boundary layer experiment and Lagrangian wind data from tetroon trajectories near Las Vegas and Idaho Falls are analyzed. At extreme values of $u'(t)$ for the Eulerian data, $u'(t+\tau)$ tends to be slightly less than that predicted by the above relationship. An application of this formula to the calculation of diffusion yields results in agreement with Taylor's theory.

1. Introduction

The main purpose of this research is the study of methods of estimating Lagrangian or Eulerian wind fluctuations at one time based on a knowledge of wind fluctuations at some previous time. Smith (1968), in a study of the conditioned motion of fluid particles, introduced the assumption that the Lagrangian turbulent fluctuation u' of a given fluid parcel at any time $t+\tau$ is linearly related to the turbulent fluctuation at some previous time, t i.e.,

$$u'(t+\tau)=u'(t)R(\tau)+u''(t). \quad (1)$$

The proportionality factor $R(\tau)$ is the autocorrelation coefficient at time lag τ. This assumption is potentially very useful in simulating the time variation of turbulent velocity along an air parcel trajectory. The last term, $u''(t)$, is a random component of the turbulence, assumed to be independent of $u'(t)$. The standard deviation $\sigma_{u''}$ of the random component must be defined by the relation

$$\sigma_{u''}=\sigma_{u'}[1-R^2(\tau)]^{\frac{1}{2}} \quad (2)$$

in order that turbulent energy $\sigma_{u'}^2$ be conserved with time. There are not many Lagrangian turbulence data available to test this assumption. Smith (1968) analyzed a few geostrophic wind trajectories which suggested that $u'(t+\tau)$ was proportional to $u'(t)$, and that $\sigma_{u''}$ was roughly independent of $u'(t)$. By analyzing wind speed data for a single run from an anemometer suspended from a tethered balloon, Smith (1973) also determined that $u'(t+\tau)$ was proportional to $u'(t)$ in all cases except for the extreme 1% at the tails of the wind speed distribution. In the region of extreme turbulence fluctuations, wind speed fluctuations tended to revert toward the mean value to a degree greater than is suggested by Eq. (1).

These concepts will be tested further in this paper using recent Eulerian wind data from the Minnesota boundary layer experiment and Lagrangian wind data from tetroon flights in Las Vegas and Idaho Falls. Lagrangian and Eulerian motions are assumed to be related in a way suggested by several workers, e.g., Gifford (1955) and Hay and Pasquill (1959), i.e., the Lagrangian and Eulerian correlograms and spectra are similar in shape and differ only in their time scales, denoted by T_L and T_E. The ratio T_L/T_E is commonly called β.

2. Analysis of Minnesota Eulerian wind data

During September 1973, the Air Force Cambridge Research Laboratories (AFCRL) and the British Meteorological Office (BMO) cooperated in a series of Eulerian measurements of wind and temperature in the boundary layer over flat farmland in Minnesota. The general experiment is described by Readings *et al.* (1974), a data summary is presented by Izumi and Caughey (1976), and several analyses of the data have appeared in the literature (see, e.g., Kaimal *et al.*, 1976). The wind data used in this analysis are from the BMO instruments, which are cup anemometers located at five levels between about 61 and 1220 m, held aloft by a large captive balloon and its tethering cable. These observations are analyzed together and considered to represent the mid to upper portions of the planetary boundary layer.

The nine runs listed in Table 1 were studied. Monin–Obukhov lengths, friction speeds and other Eulerian turbulence information for the unstable runs are given

TABLE 1. Minnesota runs.

Run	Unstable					Stable			
	3A1	5A1	6A1	6B1	7C1	3	4A	4B	5
Date	9/11/73	9/15/73	9/17/73	9/17/73	9/19/73	9/11/73	9/13/73	9/14/73	9/15/73
Starting time (LT)	1510	1622	1401	1652	1415	2316	2315	0426	2144

by Izumi and Caughey (1976). Each run is 75 min in length, but we used only the first two 15 min segments of a run. The recorded data represent total wind speed. Since the time interval between readings is 0.1 s, each 15 min run contains 9000 individual wind speed records. Wind speeds were moderate, ranging from 4.6 to 11.6 m s^{-1}, and turbulence intensities $\sigma_{u'}/\bar{u}$ were about 0.15 for the unstable runs and about 0.07 for the stable runs.

a. Test of the assumption $u'(t+\tau)=u'(t)R(\tau)+u''(t)$

To test the linearity assumption, initial wind fluctuations $u'(t)$ were grouped into 30 ranges from $-5\sigma_{u'}$ to $+5\sigma_{u'}$, each range or interval covering $\sigma_{u'}/3$. If, for example, $\sigma_{u'}$ were 1 m s^{-1}, then the ranges would be

Range 1: -5.00 m $s^{-1} < u' \leqslant -4.67$ m s^{-1}
Range 2: $-4.67 < u' \leqslant -4.33$
⋮
Range 15: $-0.33 < u' \leqslant 0$
Range 16: $0 < u' \leqslant 0.33$
⋮
Range 29: $4.33 < u' \leqslant 4.67$
Range 30: 4.67 m $s^{-1} < u' \leqslant 5.00$ m s^{-1}

Each wind fluctuation $u'(t)$ is placed into one of the 30 ranges, and the observed $u'(t+\tau)$ is found from the data record, using time lags τ of 1, 5, 10, 30 and 60 s. The $u'(t+\tau)$ values for each range of $u'(t)$ and each time lag τ are then averaged [giving $\overline{u'(t+\tau)|u'(t)}$], and the standard deviation of the random component of turbulence $\sigma_{u''}$ is calculated. The notation $\overline{u'(t+\tau)|u'(t)}$ refers to the average value of $u'(t+\tau)$, given $u'(t)$. For ease in comparing various runs, all fluctuations u' are normalized by the standard deviation of the turbulent fluctuations $\sigma_{u'}$.

In order to more efficiently present the observations used to test the linearity implied by Eq. (1), all runs with correlation coefficients $R(\tau)$ in certain narrow ranges were grouped together. Fig. 1 shows normalized values of $\overline{u'(t+\tau)|u'(t)}$ as a function of $u'(t)/\sigma_{u'}$ for 45 unstable runs with $R(\tau)>0.85$. The average $R(\tau)$ for the 45 runs is 0.89. All correlations $R(\tau)>0.85$ are found at time lag τ equal to 1, 5 or 10 s. Note that in the region $-1.5<u'(t)/\sigma_{u'}<1.5$, which contains ~86% of the data points, the data fall along a straight line with slope exactly equal to $R(\tau)$, as suggested by (1), the basic assumption of this paper. At extreme values of $u'(t)$, where $|u'(t)|/\sigma_{u'}>1.5$, the curve becomes slightly S shaped, as Smith (1973) found with his Eulerian data, and the fluctuations $u'(t+\tau)$ are slightly less than what Eq. (1) would predict. There is much less certainty in the extreme points because comparatively few data records are represented.

Four stable runs were also analyzed, to see if there was any dependence of the linearity relationship on stability. The fluctuation $(\overline{u'(t+\tau)|u'(t)})/\sigma_{u'}$ is plotted as a function of $u'(t)/\sigma_{u'}$ for correlations $R(\tau)$ between 0.8 and 0.9 in Fig. 2. The stable curve is slightly more linear at the extremes than the unstable curve, and the basic linearity assumption [Eq. (1)] is indeed verified by these data over most of the range of $u'(t)$.

Similar plots were made for correlation ranges $0.7<R<0.8$, $0.6<R<0.7$, etc., for both the stable and unstable observations. The curves are linear with

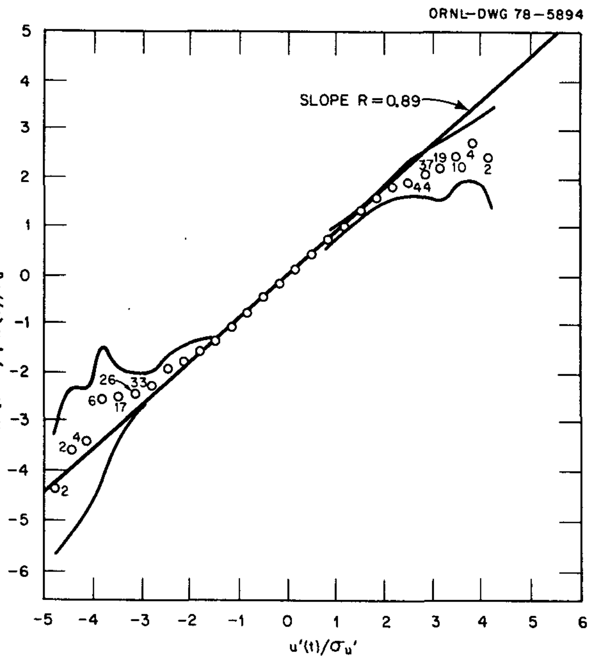

FIG. 1. Normalized average $[\overline{u'(t+\tau)|u'(t)}]/\sigma_{u'}$ of the wind fluctuation at any time $t+\tau$ plotted versus the normalized initial wind fluctuation $u'(t)/\sigma_{u'}$ at time t. 45 unstable Minnesota runs with $R(\tau)>0.85$ are used. $\overline{R(\tau)}=0.89$. Where numbers appear beneath the point, they indicate the number of cases represented (if less than 45). The curved line represents $\pm\sigma$ for the 45 cases. The notation $\overline{u'(t+\tau)|u'(t)}$ refers to the average value of $u'(t+\tau)$, given $u'(t)$.

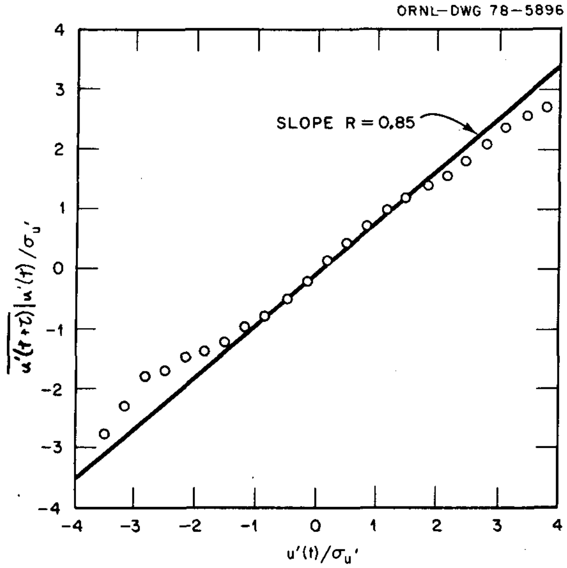

FIG. 2. As in Fig. 1 except that four stable Minnesota runs with $0.8<R(\tau)<0.9$ are used. Time lags of 1, 5 or 10 s are represented.

slope $R(t)$ over the range $1.5\sigma_{u'}<u'(t)<1.5\sigma_{u'}$, in agreement with Figs. 1 and 2, and also have a slight S shape at extreme values of $u'(t)$ outside of this range.

b. Shape of the conditional probability distribution function

The distribution $P[u'(t+\tau)|u'(t)]$, that is, the probability that the wind speed fluctuation at time $t+\tau$ will have a certain value under the condition that the fluctuation at time t is specified, was calculated for various initial values of $u'(t)$. Fig. 3 is a typical example of such a distribution, obtained from run 7, with $u'(t)$ in the range $-1.67\sigma_{u'}$ to $-1.33\sigma_{u'}$. A theoretical Gaussian curve is drawn as a dashed line. The observed frequency of occurrence of $u'(t+\tau)$ is fairly close to the Gaussian curve, and it is expected that agreement would improve if the size of the data sample were increased. All the plotted distributions of this type were roughly Gaussian, exhibiting little evident skewness. The standard deviation of each conditional distribution curve equals $\sigma_{u''}$, which is the previously defined standard deviation of the random component of turbulence.

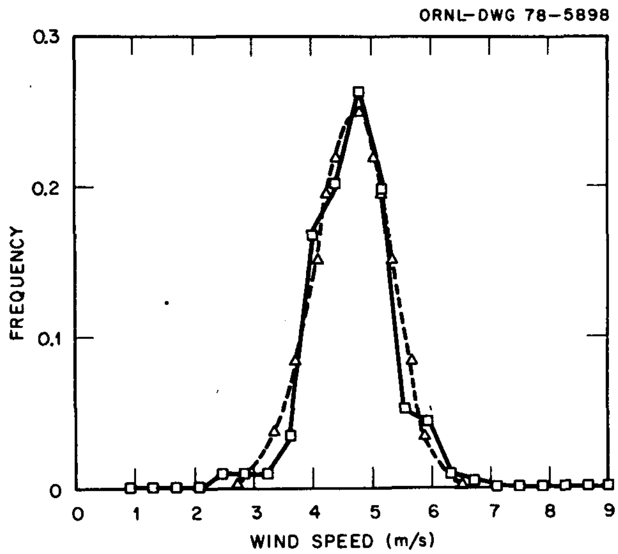

FIG. 3. Observed conditional probability distribution function $P[u'(t+\tau)|u'(t)]$ for $-5/3<u'(t)/\sigma_{u'}<-4/3$, Minnesota run 7, level 1. The squares connected by a solid line are the observed points and the triangles connected by a dashed line are points following a Gaussian or normal distribution. $\bar{u}=5.69$ m s^{-1}, $\sigma_{u''}=0.63$ m s^{-1}, $\tau=1$ s, $R(\tau)=0.89$.

c. Test of the assumption that $\sigma_{u''}$ is independent of $u'(t)$

Smith (1968) presented a few Lagrangian data from barotropic wind trajectories that verified the independence of $\sigma_{u''}$ and u'. In Fig. 4 the normalized ratios $\sigma_{u''}(\text{range})/\overline{\sigma_{u''}}$ are plotted as a function of $u'(t)/\sigma_{u'}$ for unstable Eulerian runs at Minnesota. The primed variable is the turbulent wind speed fluctuation, and the double primed variable is the random component of the total turbulent fluctuation, as defined in Eq. (1). The variable $\overline{\sigma_{u''}}$ is the weighted average standard deviation of 30 ranges in each run. Separate points are plotted for each of the seven correlation (R) groups, and the average curve is drawn as a solid line. In the interval $-2<u'(t)/\sigma_{u'}<2$,

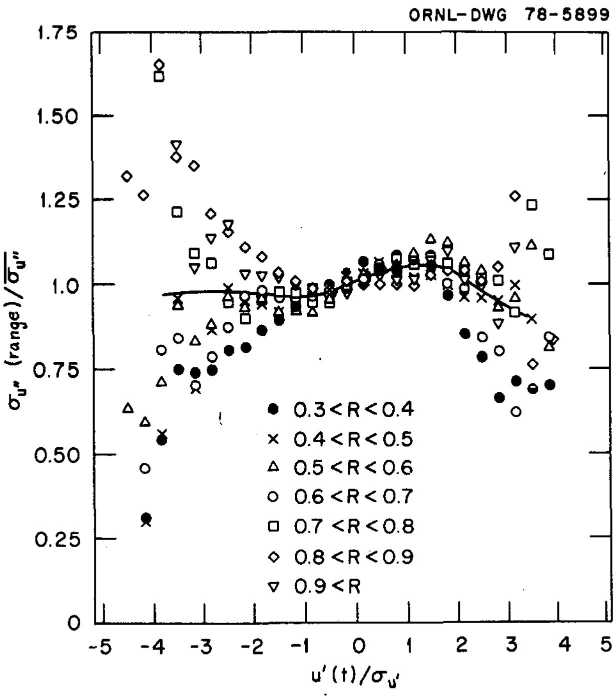

FIG. 4. Variation of the ratio $\sigma_{u''}(\text{range})/\overline{\sigma_{u''}}$ with initial normalized fluctuations $u'(t)/\sigma_{u'}$ for unstable Minnesota runs. Data are separated also into seven groups of $R(\tau)$. The solid line is the best-fit line to the data points.

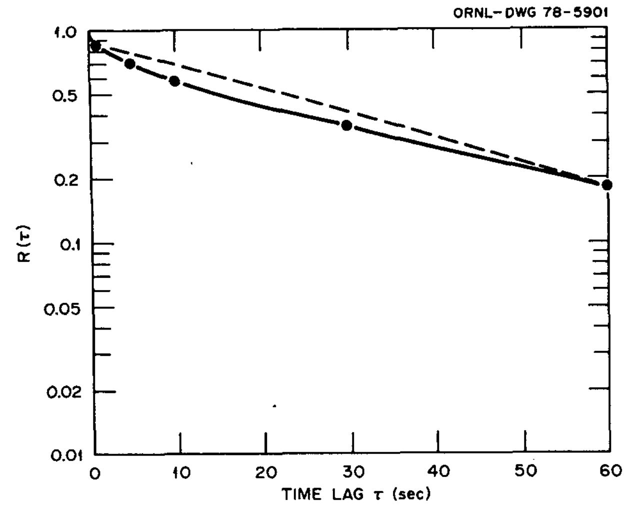

FIG. 5. Autocorrelation coefficient $R(\tau)$ versus time lag τ averaged over all unstable Minnesota runs. A dashed straight line is drawn between the points for τ equal to 1 and 60 s in order to illustrate the departure of the curve from a straight line.

there is a tendency for $\sigma_{u''}$ to be a few percent less than the average for $u'(t)<0$, and a few percent higher than the average for $u'(t)>0$.

On the average, there are slightly reduced values of $\sigma_{u''}$ at the extremes. It is also noticeable that the normalized $\sigma_{u''}$ tends to be larger at the extremes of $u'(t)$ for high correlations $R(\tau)$ than for low correlations. It can be concluded that $\sigma_{u''}$ is nearly independent ($\pm 10\%$) of $u'(t)$ for $-2<u'(t)/\sigma_{u'}<2$, i.e., for 95% of the data.

d. Shape of the correlation function $R(\tau)$

The average correlation $R(\tau)$ for the unstable Minnesota runs is plotted on a logarithmic ordinate in Fig. 5. The observed values curve slightly below a straight line representing the formula $R(\tau)=e^{-\tau/33\ \mathrm{s}}$. It can be concluded that the magnitude of $R(\tau)$ can be approximated by an exponential function to within $\sim 20\%$ for the range of time lags studied in this paper.

3. Analysis of Las Vegas Lagrangian wind data

The basic assumptions in this paper were introduced in the framework of Lagrangian flows. Angell *et al.* (1971) published analyses of radar observations of 35 constant volume balloons (tetroons) flown at heights of 400–500 m past the 460 m BREN tower at the Nevada Test Site during the spring of 1968. Turbulent vertical speed fluctuations were estimated from instantaneous tetroon positions observed every $\frac{1}{2}$ min during flights with mean durations of about 1 or 2 h. Since each run contains only 100 or 200 data records, the results of these analyses will not be as statistically significant as the results of the analysis of the Eulerian wind observations at Minnesota where thousands of data records were available for each run. But the tetroon data from Las Vegas and other tetroon data from Idaho Falls to be discussed in the next section are among the only atmospheric Lagrangian wind data currently available. Wind speeds during the Las Vegas runs ranged from 4 to 10 m s^{-1} and $\sigma_{w'}$ ranged from near zero to more than 2 m s^{-1}. The experiments were carried out during the day.

Correlations dropped off to zero at a time lag of $\sim$4 min for these data (Fig. 6). The results of two runs with relatively large correlations are given in Fig. 7, where the averaged conditional fluctuation $\overline{w'(t+\frac{1}{2}\ \mathrm{min})|w'(t)}$ is plotted as a function of $w'(t)$. The slope of the curves equals $R(\frac{1}{2}\ \mathrm{min})$, as suggested by (1), and there is no S shape to the extreme ends of the curve.

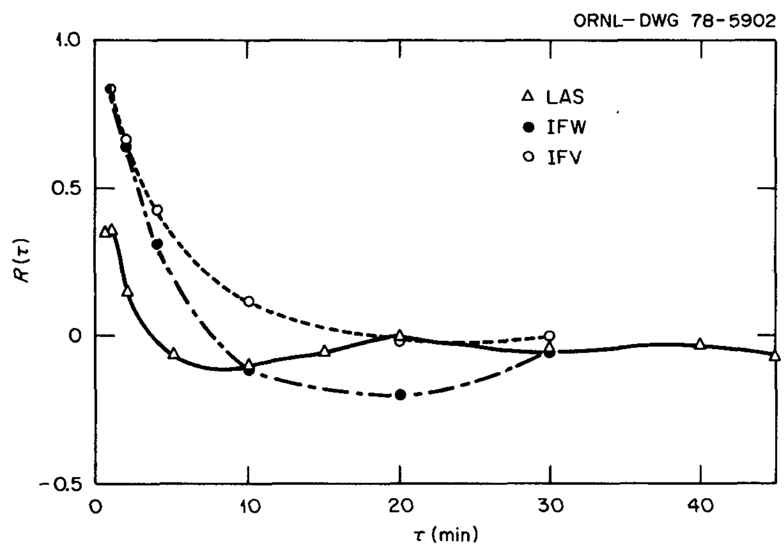

FIG. 6. As in Fig. 5 except averaged over all Las Vegas w' and Idaho Falls w' and v' runs. Lagrangian tetroon data.

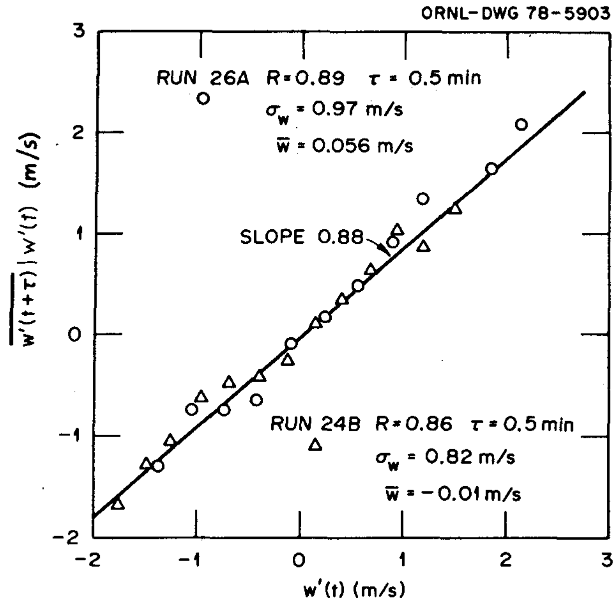

FIG. 7. Average vertical velocity fluctuation $\overline{w'(t+\tau)}|w'(t)$ at any time $t+\tau$ plotted versus the fluctuation $w'(t)$ at time t, for two unstable Las Vegas runs. Lagrangian tetroon data.

An indication that $\sigma_{w''}$ is independent of w' is provided by Fig. 8 for these same two runs. There is much scatter, but there seems to be little dependence on w' evidenced by these results.

4. Analysis of Idaho Falls Lagrangian wind data

Nearly 100 tetroon flights were made during July 1966 at Idaho Falls, with the purpose of studying helical circulations in the planetary boundary layer (Angell *et al.*, 1968). Consequently, these data all represent convective daytime situations. Velocity estimates were made from instantaneous tetroon positions

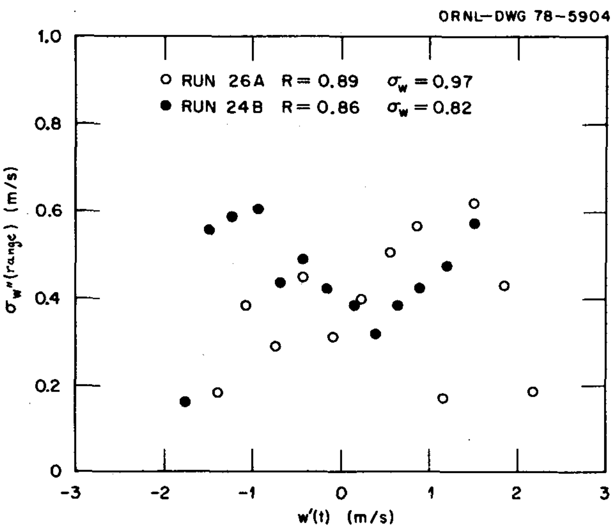

FIG. 8. Random turbulent fluctuation $\sigma_{w''}$ for each range of $w'(t)$ plotted versus $w'(t)$, for two unstable Las Vegas Lagrangian tetroon runs.

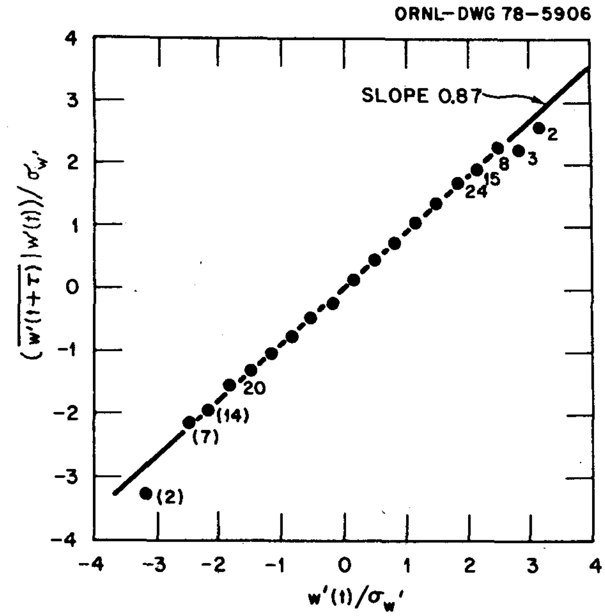

FIG. 9. Normalized average $[\overline{w'(t+\tau)}|w'(t)]/\sigma_{w'}$ of the vertical wind fluctuations at any time $t+\tau$ plotted versus the normalized initial fluctuation $w'(t)/\sigma_{w'}$ at time t. 25 Lagrangian tetroon runs from Idaho Falls with $R(\tau)>0.8$ are used. Where numbers appear beneath the point, they indicate the number of runs represented (if less than 25). The straight line has a slope equal to the average correlation $R(\tau)$.

recorded every minute during the runs, which lasted ~2 h. Mean wind speeds ranged from 6.7 to 13.7 m s^{-1} and $\sigma_{u'}$ was about 2.0 m s^{-1}. The data were analyzed

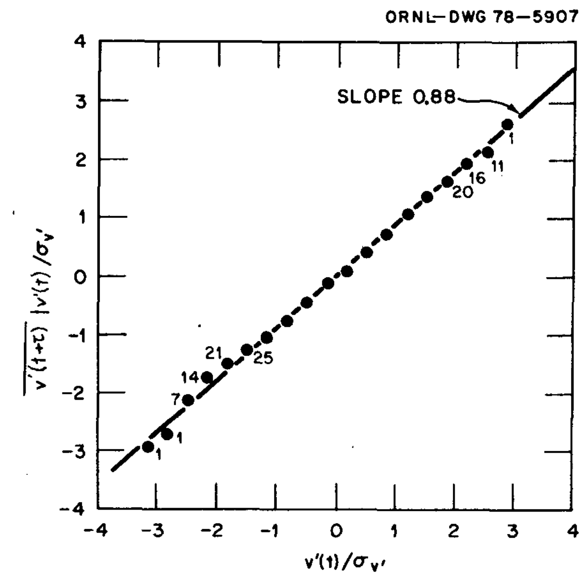

FIG. 10. Normalized average $([\overline{v'(t+\tau)}|v'(t)]/\sigma_{v'}$ of the lateral wind fluctuations at any time $t+\tau$ plotted versus the normalized initial fluctuation $v'(t)/\sigma_{v'}$ at time t. 27 Lagrangian tetroon runs from Idaho Falls with $R(\tau)>0.8$ are used. Where numbers appear beneath the point, they indicate the number of runs represented (if less than 27). The straight line has a slope equal to the average correlation $R(\tau)$.

for variations in the lateral and vertical components of the turbulent wind fluctuations, v' and w', respectively. The average correlation curves $R(\tau)$ for the 25 w' runs and the 28 v' runs are compared in Fig. 6 with the Las Vegas correlation curve, showing that the turbulence time scale is two to four times larger in the Idaho Falls experiment. Also, it is seen that $R(\tau)$ is negative for most time lags beyond about 10 min.

a. Test of the assumption $v'(t+\tau)=v'(t)R(\tau)+v''(t)$

Figs. 9 and 10 display values of $\overline{(w'(t+\tau)}|w'(t))/\sigma_{w'}$ and $\overline{(v'(t+\tau)}|v'(t))/\sigma_{v'}$ as functions of $w'(t)/\sigma_{w'}$ and $v'(t)/\sigma_{v'}$, respectively, for all runs and time lags such that the correlation coefficient $R(\tau)>0.8$. The observations fall nearly exactly on a straight line with slope equal to the average $R(\tau)$ for both sets of data. There are no systematic departures from the straight line at extreme values of turbulent fluctuations. All the Lagrangian data analyzed are characterized by agreement with the assumption $\overline{v'(t+\tau)}|v'(t)=v'(t)R(\tau)$ over the entire range of $v'(t)$.

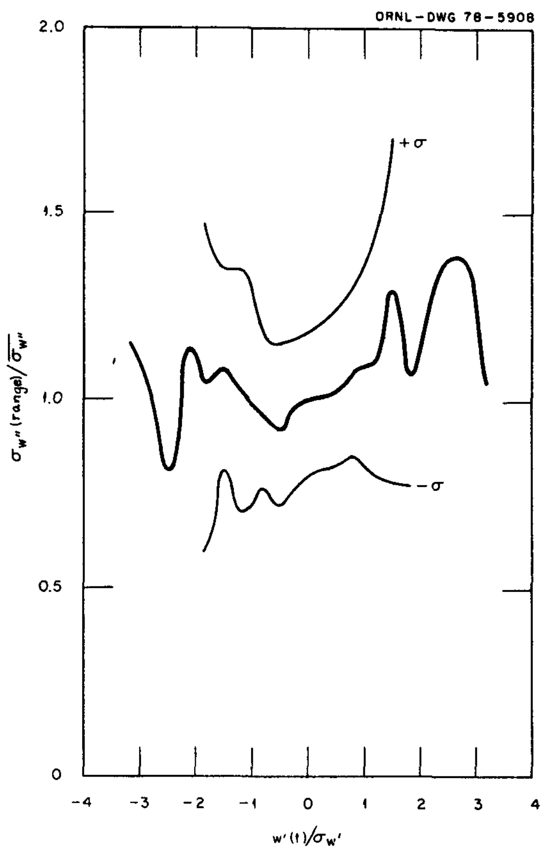

FIG. 11. Variation of the ratio $\sigma_{w''}(\text{range})/\overline{\sigma_{w''}}$ with initial normalized fluctuation $w'(t)/\sigma_{w'}$ for 25 Idaho Falls Lagrangian tetroon runs with $R(\tau)>0.8$. The thin lines represent $\pm\sigma$ for each range or value of $w'(t)/\sigma_{w'}$.

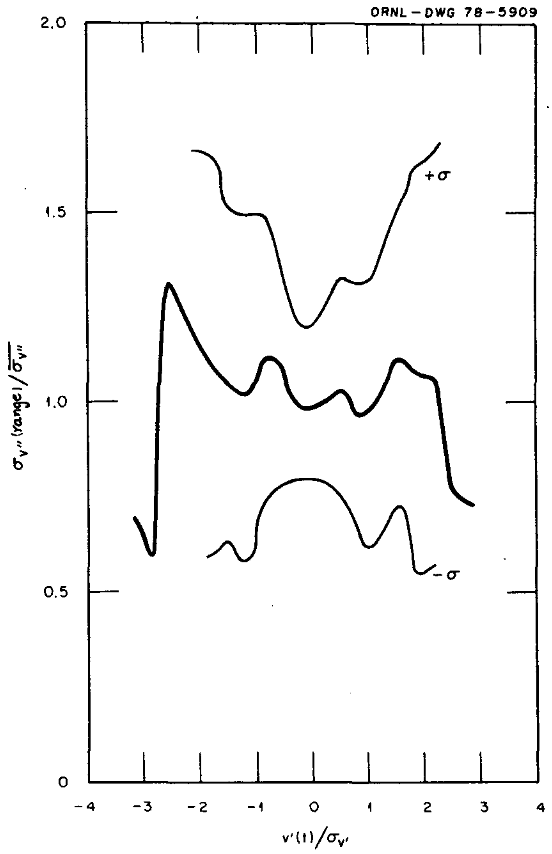

FIG. 12. Variation of the ratio $\sigma_{v''}(\text{range})/\overline{\sigma_{v''}}$ with initial normalized fluctuation $v(t)/\sigma_{v'}$ for 27 Idaho Falls Lagrangian tetroon runs with $R(\tau)>0.8$. The thin lines represent $\pm\sigma$ for each range or value of $v'(t)/\sigma_{v'}$.

b. Test of the assumption that $\sigma_{v''}$ *is independent of* $v'(t)$

The standard deviations $\sigma_{v''}$ and $\sigma_{w''}$ computed for each of the 30 ranges of v' and w' are normalized by the weighted-average $\overline{\sigma_{v''}}$ and $\overline{\sigma_{w''}}$ and plotted versus $v'(t)$ and $w'(t)$ in Figs. 11 and 12, respectively. All runs are used in these figures. There is no clear dependence of the normalized $\sigma_{v''}$ and $\sigma_{w''}$ values as a function of initial turbulent fluctuations.

5. Example of diffusion calculation made using the linearity assumption

To test the applicability of the linearity assumption to diffusion calculations, a simple computer experiment was run in which the trajectories of 1000 particles released from a single point were followed in a uniform wind field. At times up to 1000 min after release, the standard deviation σ of the crosswind position of the 1000 particles was calculated. Eq. (1) $[u'(t+\tau)=u'(t)R(\tau)+u'(t)]$ was used to generate turbulent fluctuations. At the first time step, each u' was chosen randomly from a Gaussian distribution with standard deviation $\sigma_{u'}$. The distribution of the

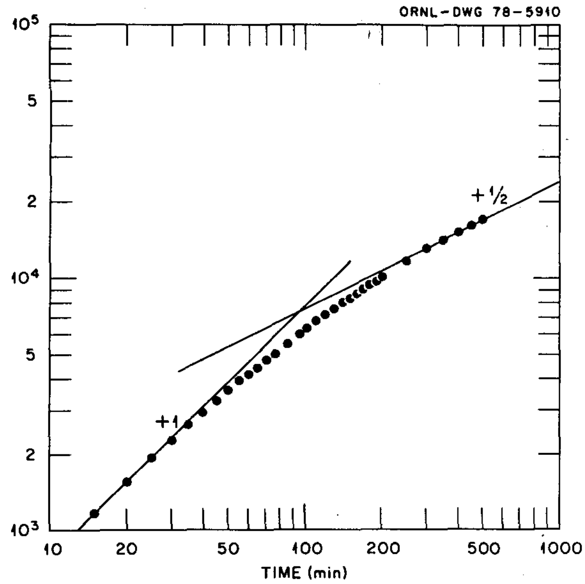

FIG. 13. Dotted line is the standard deviation σ of the spread of 1000 particles from a fixed axis as a function of time after release. The formula $u'(t+\tau)=u'(t)R(\tau)+u''(t)$ is used to generate the particle trajectories, where time step τ is assumed to be 5 minutes and $R(\tau)$ is assumed to be 0.9. The curve is asymptotic to lines representing power laws with slopes 1 and $\frac{1}{2}$, which meet at time $=2T$, where T is the time scale in $R(\tau)=e^{-\tau/T}$.

random fluctuation u'' at subsequent times was assumed to be Gaussian with zero mean and variance $\sigma_{u''}^2=\sigma_{u'}^2[1-R^2(\tau)]$. The time step was 5 min and it was assumed that R(5 min) equals 0.9. The resulting variation of the standard deviation σ of particle position with time, plotted in Fig. 13, shows a smooth transition from $\sigma \propto t$ at small times ($t \ll T$) to $\sigma \propto t^{\frac{1}{2}}$ at large times ($t \gg T$). This curve coincides almost exactly with the solution to Taylor's diffusion equation for an exponential correlogram $[R(\tau)=\exp(-\tau/T)]$:

$$\sigma^2=2\sigma_v{}^2T^2[t/T-1+\exp(-t/T)], \quad (3)$$

where the time scale T equals 50 min. With this time scale, R(5 min) $=0.9$ as assumed above.

For this simple example, the computer approach is very time-consuming when compared with the analytical solution in Eq. (3). Consequently, the computer application of the linearity assumption will be practical only in situations where standard formulas, such as the Gaussian plume formula or analytical solutions to Taylor's equation do not apply. Examples of complex situations where this approach would be valid are sea breeze flow, flow around rough terrain, or any other situation where mean winds are not uniform. In these cases, an observed or predicted mean wind field plus the application of the linearity assumption will permit calculation of particle trajectories and diffusion.

6. Further discussion

The linearity assumption

$$u'(t+\tau)=u'(t)R(\tau)+u''(t)$$

has been verified using sets of Eulerian and Lagrangian wind data. One feature of this study that is not easily explained is that the $u'(t+\tau)$ versus $u'(t)$ curve is a straight line for the Lagrangian data but tends to be slightly S shaped at the extremes of the Eulerian data. It may be that extreme Eulerian turbulence fluctuations are due to relatively small eddies which are not as persistent as the rest of the turbulence structure. Kaimal (1978) suggests that eddies of different sizes are not translated with equal velocities.

This analysis is being repeated using concurrent Eulerian-Lagrangian measurements from the September 1978 PHOENIX Experiment near Boulder, Colorado. Tower-mounted anemometers will give fixed-point Eulerian readings, an airplane with turbulence instrumentation will give Eulerian-space measurements, and radar tracking of tetroons will give Lagrangian turbulence measurements. These measurements should yield a wealth of information about this hypothesis, as well as other information about the structure of Eulerian and Lagrangian turbulence.

Acknowledgments. The Minnesota data were supplied by Duane Haugen of NOAA's Wave Propagation Laboratory in Boulder, Colorado. Tetroon data were supplied by Walter Hoecker and James Angell of NOAA's Air Resources Laboratory in Silver Spring, Maryland. Discussions with Frank Gifford and Carmen Nappo of this laboratory and F. B. Smith of the British Meteorological Office have helped to clarify questions concerning the structure of turbulence. H. F. Snodgrass of this laboratory carried out most of the computer operations with the data.

This work was performed under an agreement between the National Oceanic and Atmospheric Administration and the Department of Energy.

REFERENCES

Angell, J. K., D. H. Pack and C. R. Dickson, 1968: A Lagrangian study of helical circulations in the planetary boundary layer. *J. Atmos. Sci.*, **25**, 707–717.

——, —— and N. Delver, 1971: Lagrangian-Eulerian time-scale ratios estimated from constant volume balloon flights past a tall tower. *Quart. J. Roy. Meteor. Soc.*, **97**, 87–92.

Gifford, F. A., 1955: A simultaneous Lagrangian-Eulerian turbulence experiment. *Mon. Wea. Rev.*, **83**, 293–301.

Hay, J. S., and F. Pasquill, 1959: Diffusion from a continuous source in relation to the spectrum and scale of turbulence. *Atmospheric Diffusion and Air Pollution*, F. N. Frenkiel and P. A. Shephard, Eds., *Advances in Geophysics*, Vol. 6, Academic Press, 345 pp.

Izumi, Y., and J. S. Caughey, 1976: Minnesota 1973 atmospheric boundary layer experiment data report. AFCRL-TR-76-0038, Air Force Cambridge Res. Lab., Hanscon AFB, MA 01731, 28 pp.

Kaimal, J. C., 1978: Horizontal velocity spectra in an unstable surface layer. *J. Atmos. Sci.*, **35**, 18–24.

——, J. C. Wyngaard, D. A. Haugen, O. R. Coté and Y. Izumi, 1976: Turbulence structure in the convective boundary layer. *J. Atmos. Sci.*, **33**, 2152–2169.

Pasquill, F., 1974: *Atmospheric Diffusion*, 2nd ed. Halsted Press, 429 pp.

Readings, C. J., and H. E. Butler, 1972: The measurement of atmospheric turbulence from a captive balloon. *Meteor. Mag.*, **101**, 286–298.

——, D. A. Haugen and J. C. Kaimal, 1974: The 1973 Minnesota atmospheric boundary layer experiment. *Weather*, **29**, 309–312.

Smith, F. B., 1968: Conditioned particle motion in a homogeneous turbulent field. *Atmos. Environ.*, **2**, 491–508.

——, 1973: The equation of diffusion for a realistic homogeneous atmosphere. TDN No. 39, Meteor. Office, Boundary-Layer Res. Br., Bracknell, UK, 19 pp.